Flexural Behavior of Lean Duplex Stainless Steel Welded I-section

Takao MIYOSHI*

ABSTRACT

The initial material cost of stainless steel is mainly affected by the nickel content. Especially, the austenitic grade JIS SUS304, which is most commonly adopted in the stainless steel family, has never been used as structural members of a bridge in Japan, because it has around 8 % nickel content. The recently developed lean duplex stainless steel has around 1.5% nickel content. Although it has far lower nickel content in comparison with SUS304, its corrosion resistance is equivalent to SUS304. SUS821L1 was standardized under JIS G 4304: 2015 as a lean duplex stainless steel in Japan. SUS821L1 contributes to reducing the initial material cost of infrastructures as well as the maintenance cost for their repainting. This study focuses on the application of SUS821L1 to I-section main-girder of the small-scale bridges and aims to investigate flexural behavior of SUS821L1 welded I-section. In order to assess the ultimate flexural strength and the element interaction between the web and flanges, parametric studies regarding the web and flange plate slenderness parameters are carried out using finite element method. Numerical results are compared with the flexural strength and limiting element slenderness parameters specified in existing design standards. Based on the comparison, the limiting element slenderness parameter for yielding is proposed by taking into account the element interaction.

KEY WORDS: Lean duplex stainless steel, welded I-section, ultimate strength, element interaction

1. Introduction

Although the nickel contributes to improvement the corrosion resistance of structural steel, its price is high in comparison with many other alloying elements because of its rarity. Therefore, the initial material cost of stainless steel is mainly affected by its nickel content. Austenitic grade JIS SUS304, which is most commonly adopted in the stainless steel family, has around 8 % nickel content. Many bridges using structural carbon steel have been constructed in Japan. On the other hand, bridges using SUS304 have never been constructed in Japan, because initial material cost of SUS304 is much higher than that of structural carbon steel. However, the recently developed lean duplex stainless steel has around 1.5 % nickel content. Despite the low nickel content, its corrosion resistance is similar to that of SUS304. SUS821L1 was standardized under JIS G 4304: 2015 as a lean duplex stainless steel in Japan. The initial material cost of SUS821L1 is relatively low within stainless steel because of its low nickel content. Consequently, structural application of SUS821L1 to infrastructures contributes to reducing of their life cycle cost, laborsaving of their maintenance work and achieving their long service life. This study focuses on the application of SUS821L1 to I-section main-girder of the small-scale bridges.

Existing studies on structural behavior of SUS821L1 have been reported with regard to the stress-strain relationship, residual stresses and geometric imperfections of the welded I-section[1), 2)], ultimate strength of the plate elements[3)] and welded H-section stub-columns [4)]. However, there are few studies on the flexural strength of SUS821L1 welded I-section.

According to an existing study on flexural behavior of carbon steel I-section[5)], it has been revealed that the element interaction between the web and flanges affects the ultimate flexural behavior and that the flexural strength is evaluated

*Department of civil engineering

rationally by taking into account its interaction. Therefore, SUS821L1 welded I-section is expected to reduce its weight and plate thickness by effective utilization of the element interaction. However, the element interaction between the web and flanges of SUS821L1 welded I-section has not been made clear yet.

This study aims to investigate the ultimate strength and the element interaction between the web and flanges of SUS821L1 welded biaxial symmetric I-section under uniform bending. Parametric studies were carried out to assess influence of the web and flange plate slenderness parameters on the flexural behavior using FEM computer program developed by authors[6]. Numerical results were compared with the flexural strength and the web and flange limiting slenderness parameters specified in existing design standards[7), 8)]. Based on the comparison, the limiting plate slenderness parameter for yielding is proposed by taking into account the element interaction.

2. Key parameters that affect flexural behavior

It is well known that the web slenderness parameter λ_{pw} and the flange slenderness parameter λ_{pf} of thin-walled structures with I-shaped cross-section significantly affects the ultimate flexural behavior. λ_{pw} and λ_{pf} are given by Eqs. (1) and (2), respectively.

$$\lambda_{pw} = \frac{h_w}{t_w}\sqrt{\frac{12(1-\nu^2)}{k_w\pi^2}\frac{\sigma_{0.2}}{E}} \quad (1)$$

$$\lambda_{pf} = \frac{b_f}{t_f}\sqrt{\frac{12(1-\nu^2)}{k_f\pi^2}\frac{\sigma_{0.2}}{E}} \quad (2)$$

where h_w is the web width, t_w is the plate thickness of the web, $\sigma_{0.2}$ is the material 0.2% proof stress, ν is Poisson's ratio, E is the elastic modulus, k_w is the buckling coefficient of the web (assumed as a constant value of 23.9), b_f is the outstanding width of the flange, t_f is the plate thickness of the flange, and k_w is the buckling coefficient (assumed as a constant value of 0.43). Symbols for geometry of I-section under uniform bending are defined in Fig.1.

Other parameters that affect flexural behavior are the ratio of the flange width to the depth of the web s (= b/h_w), cross-sectional area ratio of the web and flange ρ = A_w/A_f, shape factor for the cross-section k (= W_p/W_e), and aspect ratio of the web α_w (= a/h_w)[5], in which A_w and A_f are cross-sectional area of the web and flange, respectively, W_p is the plastic section modulus, and W_e is the elastic section

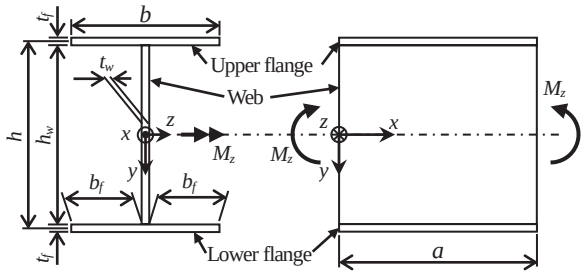

Fig.1 Schematic view of biaxial symmetric I-section

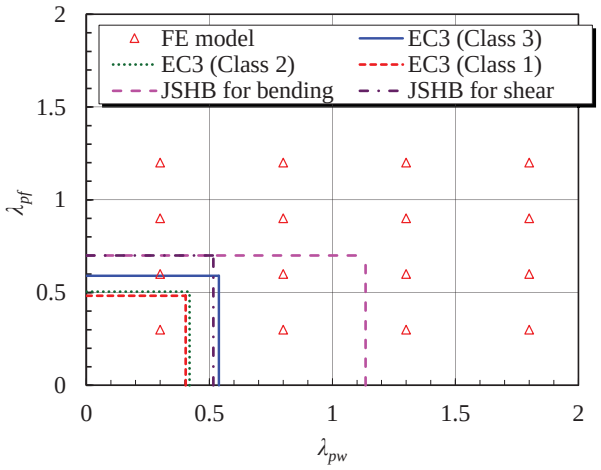

Fig.2 Relationship between flange and web slenderness

modulus. However, when t_f and t_w are enough small compared to h_w and b, 2 of these parameters are correlated with other parameters as follows.

$$\frac{\lambda_{pf}}{\lambda_{pw}} = 3.75s^2\rho \quad (3)$$

$$k = \frac{1+\rho/4}{1+\rho/6} \quad (4)$$

Therefore, λ_{pw}, λ_{pf},ρ and α_w were selected as the independent parameter in this study.

3. Parametric studies

Numerical simulations on a total of 16 SUS821L1 welded I-section under uniform bending were carried out, incorporating a wide range of web slenderness parameter λ_{pw} (0.3, 0.8, 1.3and 1.8) and flange slenderness parameter λ_{pf} (0.3, 0.6, 0.9 and 1.2). These values were based on the web and the flange limiting slendernesses of the duplex stainless steel welded I-section under uniform bending for section classification 1-3 specified in Eurocode3 (EC3)[7] and those of structural carbon steel JIS SM570 welded I-section under uniform bending for yielding specified in Japan specifications for highway bridges (JSHB)[8]. Material 0.2% proof stress of SUS821L1 almost corresponds to yield stress

of SM570. Fig.2 shows the web and flange slenderness parameters of 16 I-section and limiting slenderness parameters specified in design standards[7),8)].

From Fig.2, limiting slenderness parameters of the flange for class 3 specified in EC3 generally corresponds to that of the flange specified in JSHB. On the other hand, limiting slenderness parameters of the web for class 1-3 specified in EC3 are less than a half that of the web specified in JSHB. As a reference, the web limiting slenderness parameter of SM570 welded I-section under uniform shear and bending for yielding specified in JSHB[8)] is shown in Fig.2. It almost coincides with web limiting slenderness parameter for class 3 section.

Based on test specimens and numerical models of carbon steel welded I-section under uniform bending[5)], cross-sectional area ratio of the web and flange ρ and aspect ratio of the web α_w are assumed as 2.0 and 1.0, respectively. Variation of these parameters were considered by changing the web and flange plate thick ness t_w, t_f, flange plate width b and length a so that slenderness parameter λ_{LT} for lateral-torsional buckling of duplex stainless steel welded I-section does not exceed 0.4, which is the limiting value for yielding specified in EC3 [7)]. Table 1 shows analysis case name in parametric studies, including their dimension, slenderness parameters, design flexural strength according to EC3[7)] and so on. For instance, 13W3F denotes the analysis case of I-section with λ_{pw} = 1.3 and λ_{pf} = 0.3. Elastic modulus E, Poisson's ratio v, and material 0.2% proof stress $\sigma_{0.2}$ obtained from material coupon test[2)] for transverse direction of SUS821L1 hot-rolled plate were employed in calculation of dimension, because compressive strength of SUS821L1 simply supported and outstanding plates are able to estimate conservatively by FE analysis using their value [3)].

3・1 Stress-strain model

A modified version of the Ramberg-Osgood material model (MRO curve) was used as a stress-strain model. As shown in Fig. 3, this model is a linear elastic body up to the proportion limit σ_p, and two Ramberg-Osgood curves are connected smoothly at material 0.2% proof stress $\sigma_{0.2}$ after σ_p, as expressed by eqs.(5) and (6). Existing studies[2)-4)] have been reported that MRO curve is good agreement with material coupon test results for SUS821L1 hot-rolled plate. Values

Table 1 Dimensions, slenderness parameters, design flexural strength, and so on for each analysis case

Analysis case name	3W3F	8W3F	13W3F	18W3F	3W6F	8W6F	13W6F	18W6F	3W9F	8W9F	13W9F	18W9F	3W12F	8W12F	13W12F	18W12F
Web slenderness parameter λ_{pw}	0.3	0.8	1.3	1.8	0.3	0.8	1.3	1.8	0.3	0.8	1.3	1.8	0.3	0.8	1.3	1.8
Flange slenderness parameter λ_{pf}	0.3	0.3	0.3	0.3	0.6	0.6	0.6	0.6	0.9	0.9	0.9	0.9	1.2	1.2	1.2	1.2
Cross-sectional area ratio of the web and flange ρ	2	2	2	2	2	2	2	2	2	2	2	2	2	2	2	2
Aspect ratio of the web α_w	1	1	1	1	1	1	1	1	1	1	1	1	1	1	1	1
Width of the web h_w (mm)	300	300	300	300	300	300	300	300	300	300	300	300	300	300	300	300
Poisson's ratio v	0.24	0.24	0.24	0.24	0.24	0.24	0.24	0.24	0.24	0.24	0.24	0.24	0.24	0.24	0.24	0.24
Material 0.2% proof stress $\sigma_{0.2}$ (N/mm^2)	577	577	577	577	577	577	577	577	577	577	577	577	577	577	577	577
Elastic modulus E (N/mm^2)	213	213	213	213	213	213	213	213	213	213	213	213	213	213	213	213
Web plate thickness t_w (mm)	11	4	3	2	11	4	3	2	11	4	3	2	11	4	3	2
Cross-sectionla area of the web A_w (mm^2)	3420	1283	789	570	3420	1283	789	570	3420	1283	789	570	3420	1283	789	570
Cross-sectional area of flanges A_f (mm^2)	1710	641	395	285	1710	641	395	285	1710	641	395	285	1710	641	395	285
Outstanding width of the flange b_f (mm)	52	33	26	22	75	47	37	31	92	57	45	38	107	66	52	44
Width of the flange b (mm)	116	69	54	46	161	97	76	64	196	119	93	79	226	137	107	91
Flange plate thickness t_f (mm)	15	9	7	6	11	7	5	4	9	5	4	4	8	5	4	3
Member length a (mm)	300	300	300	300	300	300	300	300	300	300	300	300	300	300	300	300
Section classification of the web acoording to EC3	Class 1	Class 4	Class 4	Class 4	Class 1	Class 4	Class 4	Class 4	Class 1	Class 4	Class 4	Class 4	Class 1	Class 4	Class 4	Class 4
Section classification of the flanges acoording to EC3	Class 1	Class 1	Class 1	Class 1	Class 4	Class 4	Class 4	Class 4	Class 4	Class 4	Class 4	Class 4	Class 4	Class 4	Class 4	Class 4
Slenderness parameter for lateral-torsional buckling λ_{LT}	0.18	0.28	0.34	0.40	0.12	0.20	0.24	0.28	0.10	0.15	0.19	0.21	0.08	0.12	0.15	0.17
Design flexural strength according to EC3 $M_{b,Rd}$ (kNm)	444	139	79	55	394	138	79	55	349	121	68	47	312	107	59	40
Yielding moment $M_{0.2}$ (kNm)	395	148	91	66	395	148	91	66	395	148	91	66	395	148	91	66
Design flexural strength according to JSHB M_U (kNm)	395	143	85	59	395	148	89	63	244	91	56	41	137	51	32	23

obtained from the existing coupon test results[2] for transverse direction of SUS821L1 hot-rolled plate were employed as material constants of the model, as shown in Table 2.

$$\varepsilon=\begin{cases}\dfrac{\sigma}{E} & \left(0\le\sigma<\sigma_p\right)\\ \dfrac{\sigma}{E}+a_m\left(\sigma^{n1}-\sigma_p^{n1}\right) & \left(\sigma_p\le\sigma<\sigma_{0.2}\right)\\ \dfrac{\sigma}{E}+b_m\sigma+c_m+d_m\left(\sigma-\sigma_{0.2}\right)^{n1} & \left(\sigma_{0.2}\le\sigma\right)\end{cases}\quad(5)_{1\text{-}3}$$

$$a_m=\frac{0.002}{\sigma_{0.2}^{n1}-\sigma_p^{n1}},\ b_m=\frac{0.002n1\sigma_{0.2}^{n1-1}}{\sigma_{0.2}^{n1}-\sigma_p^{n1}},$$

$$c_m=\varepsilon_{0.2}-\frac{\sigma_{0.2}}{E_{0.2}},\qquad(6)_{1\text{-}4}$$

$$d_m=\frac{1}{\left(\sigma_{10}-\sigma_{0.2}\right)^{n2}}\left(\varepsilon_{10}-\varepsilon_{0.2}-\frac{\sigma_{10}-\sigma_{0.2}}{E_{0.2}}\right),$$

$$E_{0.2}=\frac{E\left(\sigma_{0.2}^{n1}-\sigma_p^{n1}\right)}{\sigma_{0.2}^{n1}-\sigma_p^{n1}+0.002n1E\sigma_{0.2}^{n1-1}}$$

where ε is the strain, σ is the stress, E is the modulus of elasticity, σ_p is the proportion limit, $n1$ and $n2$ are strain hardening exponents of the first and second curves, respectively, $\sigma_{0.2}$ is the material 0.2% proof stress, $\varepsilon_{0.2}$ is the strain at $\sigma_{0.2}$, ε_{10} is the 10% strain (=0.1), σ_{10} is the stress at 10% strain.

3・2　Numerical analysis method

Elasto-plastic finite displacement analysis was performed using an FEM program developed by authors[6]. This program has a eight-node isoparametric shell element. MRO curve is incorporated into the program.. Von mises yield function, associated flow rule and implicit stress integration scheme[12] are employed to treat elasto-plastic problem, and updated Lagrangian formulation is applied to consider geometric nonlinearity.

3・3　Finite element model

Finite element model, including boundary and loading conditions are shown in Fig.4. As shown in Fig.4, finite element model for SUS821L1 welded I-section under uniform bending has two vertical stiffeners to prevent the distortion of cross-section at the both ends. Material properties of the vertical stiffener are similar to that of I-section, and outstanding width of the stiffener is equal to that of the flanges. Plate thickness of the stiffener was determined so that its width-to-thickness ratio satisfies the limiting value for class 1 section of the welded duplex stainless steel outstanding element under uniform compression[6]. Flexural moment was applied as compulsory displacements corresponded to deformation by uniform bending.

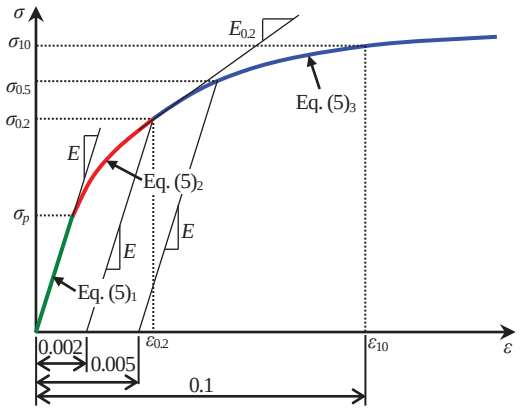

Fig.3 Schematic diagram of stress-strain model (MRO curve)

Table 2 Material constants of MRO curve

ν	E (N/mm^2)	σ_p (N/mm^2)	$\sigma_{0.2}$ (N/mm^2)	$E_{0.2}$ (N/mm^2)	σ_1 (N/mm^2)	σ_{10} (N/mm^2)	n_1	n_2
0.24	212708	388	577	31117	627	723	7.52	2.43

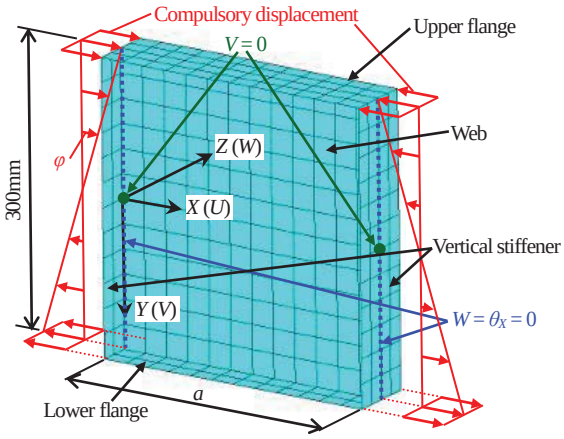

Fig.4 Finite element model

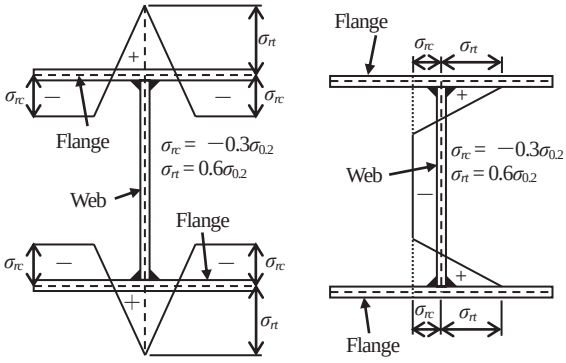

(a) Flange　　(b) Web

Fig.5 Residual stress distribution model

3・4　Residual stresses

Fig.5 shows a model of the residual stress distribution for SUS821L1 welded I-section. Shape of this model has been

used in many numerical analyses for investigating the ultimate strength of carbon steel structures [9]. Based on existing measurement results of SUS821L1 welded I-section[1), 2)], tensile residual stress peak value σ_{rt} was assumed as 0.6 times of the material 0.2% proof stress $\sigma_{0.2}$, and minimum value of compressive residual stress σ_{rc} was assumed as -0.3 times of$\sigma_{0.2}$. This model almost corresponds to existing residual stress distribution model for duplex stainless steel welded I-section proposed by Yuan et al.[10)]

3・5 Initial geometric imperfections

Initial geometric imperfection of the web and upper flange were considered as depicted in Fig.6. According to linear buckling theory[11)], if the web of I-section under uniform bending can be considered simply supported plate element, shape of initial geometric imperfection in longitudinal direction that gives minimum buckling coefficient changes in accordance with the web aspect ratio α_w. That is to say, the shape of the plate element with approximately $\alpha_w \leq 0.9$ becomes a half sine wave, and that of one with $0.9 < \alpha_w \leq 1.6$ becomes a sine wave. Because finite element models have web aspect ratioα_w = 1.0, initial geometric imperfection shape of the upper flange and web are given as eqs.(7) and (8), respectively.

$$v_0 = -\frac{h_w + t_f}{2} - \frac{2v_{0\max}}{b} z \sin\left(\frac{2\pi x}{a}\right) \quad (7)$$

$$w_0 = w_{0\max} \sin\left(\frac{2\pi x}{a}\right) \cos\left(\frac{\pi y}{h_w + t_f}\right) \quad (8)$$

where b is width of the flanges, a is the member length, v_{0max} and w_{0max} are maximum deformation deviation in accordance with the allowable value of the initial maximum deformation deviation for a carbon steel plate elements[8)]. v_{0max} and w_{0max} are represented by eqs.(9) and (10), respectively.

$$v_{0\max} = \frac{b}{200} \quad (9)$$

$$w_{0\max} = \frac{h_w + t_f}{250} \quad (10)$$

4. Analysis results

4・1 Moment versus rotation angle curves

Fig.7 shows moment versus rotation angle curves of 3W3F, 3W12F, 18W3F and 18W12F. In this figures, the vertical axis indicates the non-dimensional parameter of flexural moment divided by the yielding moment ($M/M_{0.2}$) and the lateral axis, the non-dimensional parameter of rotation angle divided by the yielding rotation angle $\varphi_{0.2}$ ($\varphi/\varphi_{0.2}$), where M

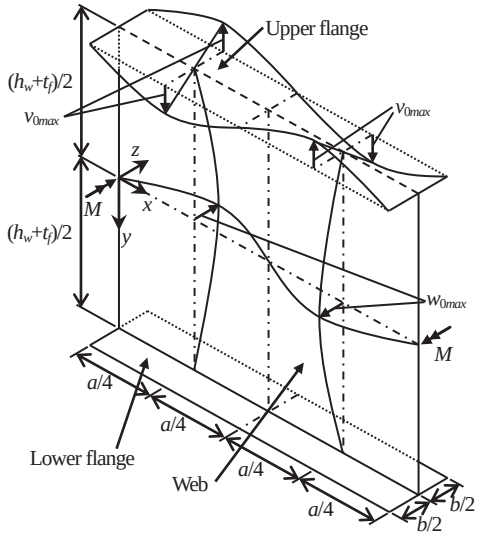

Fig.6 Schematic view of initial geometric imperfection

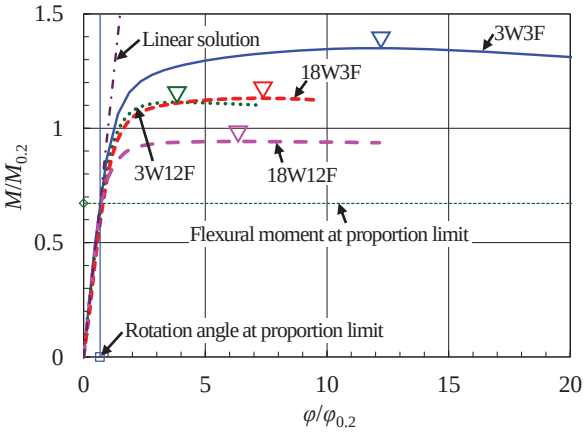

Fig.7 Moment-rotation angle curves

and φ are flexural moment and rotation angle around the z-axis, respectively, as shown in Fig.4 and 6. Inverted triangle symbol indicates a peak point for each curve. Ultimate moment M_U is defined as flexural moment at the peak point. Furthermore, the non-dimensional of flexural moment and rotation angle at proportion limit, including a linear solution are shown in the figure.

Figs.7 shows that SUS821L1 welded I-section under uniform bending exhibit a smooth curve up to the peak point and collapse gradually because of the rounded stress-strain curve.

Figs.8 (a) and (b) show the deformed shape and normalized von Mises stress ($\sigma_e/\sigma_{0.2}$) contour at the peak point of 13W9F and 3W3F, respectively, where σ_e is the von Mises stress, and $\sigma_{0.2}$ is the material 0.2% proof stress. Fig.8 (a) shows that the upper flange deforms significantly and the von Mises stress decrease considerably in the compression side of the web

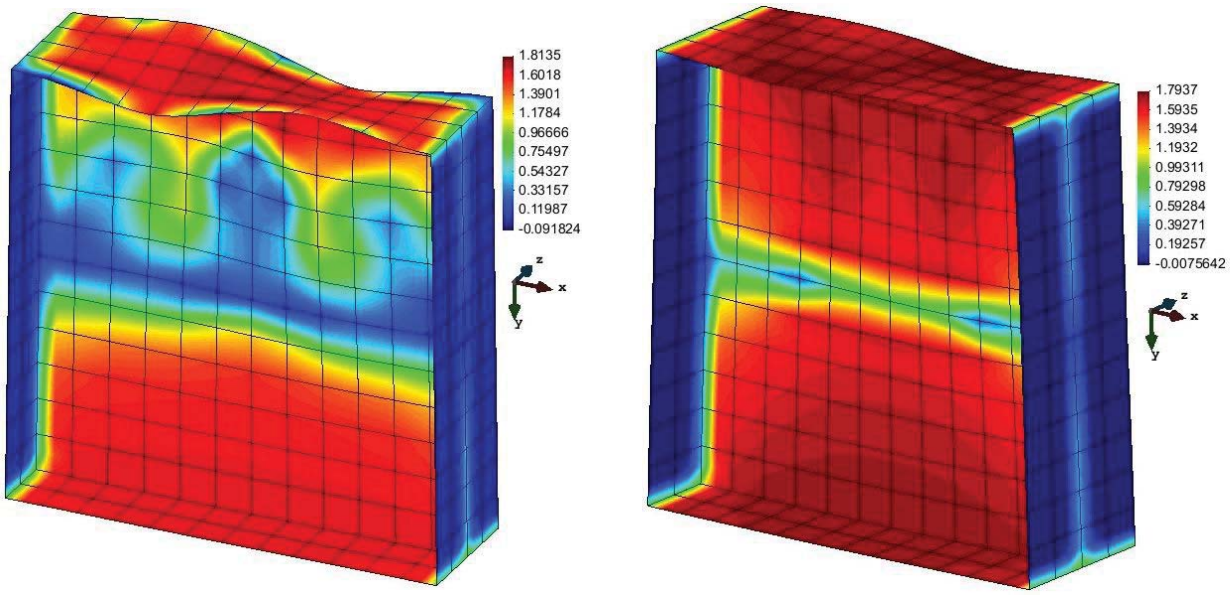

(a) 13W9F　　(b) 3W3F

Fig.8 Deformed shape and von Mises stress contour

owing to slender web and flanges. On the other hand, as shown in Fig.8 (b), stockier web and flanges provide their comparatively small deformation and high von Mises stress distribution in the compression side of the web.

4・2　Ultimate flexural strength

Table 3 shows a comparison between ultimate flexural strength obtained from FE results and design flexural strength based on rules specified in EC3[7] and JSHB[8]. Furthermore, non-dimensional flexural strength divided by design strength (A/E) and (A/J), including their average value and coefficient of variation (C.O.V.) are shown in the table.

From Table 3, the ultimate flexural moment exceeds the yielding moment except for 8W12F, 13W9F, 13W12F, 18W9F and 18W12F. Therefore, SUS821L1 I-section has considerably high flexural strength. Moreover, the design flexural strength is smaller than that of FE results. That is to say, design methods specified in EC3 and JSHB underestimate the ultimate flexural strength of SUS821L1 welded I-section. However, the method of EC3 yields accurate strength compared to that of JSHB, because mean value of A/E is smaller than that of A/J, and C.O.V. of A/E is smaller than that of A/J. For this reason, developing the design method is required for accurately estimating ultimate flexural strength of SUS821L1 welded I-section in the future.

4・3　Element interaction

Table 3 Comparison between FE results and design strength

Analysis case	$M_U/M_{0.2}$			A/E	A/J
	FEA (A)	EC3 (E)	JSHB (J)		
3W3F	1.350	1.125	1.000	1.20	1.35
3W6F	1.238	0.997	1.000	1.24	1.24
3W9F	1.164	0.883	0.617	1.32	1.89
3W12F	1.113	0.791	0.347	1.41	3.21
8W3F	1.196	0.936	0.964	1.28	1.24
8W6F	1.112	0.933	0.998	1.19	1.11
8W9F	1.031	0.817	0.617	1.26	1.67
8W12F	0.991	0.723	0.347	1.37	2.85
13W3F	1.145	0.869	0.931	1.32	1.23
13W6F	1.054	0.865	0.974	1.22	1.08
13W9F	0.980	0.747	0.617	1.31	1.59
13W12F	0.952	0.747	0.617	1.28	1.54
18W3F	1.131	0.834	0.903	1.36	1.25
18W6F	1.027	0.830	0.955	1.24	1.07
18W9F	0.969	0.710	0.617	1.37	1.57
18W12F	0.942	0.612	0.347	1.54	2.71
Mean				1.31	1.66
C.O.V.				0.066	0.391

Fig.9 shows moment versus displacement curves for analysis case 3W9F, 8W9F, 13W9F and 18W9F. In this figures, the vertical axis indicates the non-dimensional parameter of flexural moment divided by the yielding moment ($M/M_{0.2}$) and the lateral axis, the non-dimensional parameter of displacement divided by the flange plate

thickness (δ/t), where δ is the displacement along y-axis of point A and B located at the tips of the upper flange, as shown in Fig.10. t is the flange plate thickness. Inverted triangle symbol indicates the peak point for each curve.

From Fig.9, displacement at peak point increases in accordance with increase of the web plate slenderness, because the web elastically constrains deformation of the flange. Therefore, element interaction between the web and flanges of SUS821L1 welded I-section was observed.

4・4 Limiting element slenderness for yielding

Fig.11 shows relationships between web slenderness parameter λ_{pw}, flange slenderness parameter λ_{pf}, and ultimate flexural strength $M_U/M_{0.2}$ (numerical value in the parentheses), including the web and flange limiting slenderness parameters SM570 welded I-section under uniform bending for yielding specified in JSHB[8], the web and flange limiting slenderness parameters of the duplex stainless steel welded I-section under uniform bending for section classification 1-3 specified in EC3[7].

From Fig.11, ultimate flexural strength of some analysis cases which the web and flange slenderness parameters are greater than limiting slenderness parameter for class-3 section specified in EC3 exceeds 1.0. That is to say, limiting slenderness parameter for of duplex stainless steel welded I-section under uniform bending for class-3 section specified in EC3 is considerably severe as that of SUS821L1 welded I-section for yielding. Therefore, based on a counter line for yielding moment (i.e. curve that satisfies $M_U/M_{0.2} = 1$), limiting element slenderness for yielding is proposed by taking into account the element interaction between the web and flange. This curve is expressed by Eq. (11) and the curve is shown in Fig.11.

$$-0.2553\lambda_{pw}^2 + 0.0779\lambda_{pw} + 0.4558\lambda_{pf} = 1 \quad (\lambda_{pw} \le 1.8,\ \lambda_{pf} \le 1.2) \tag{11}$$

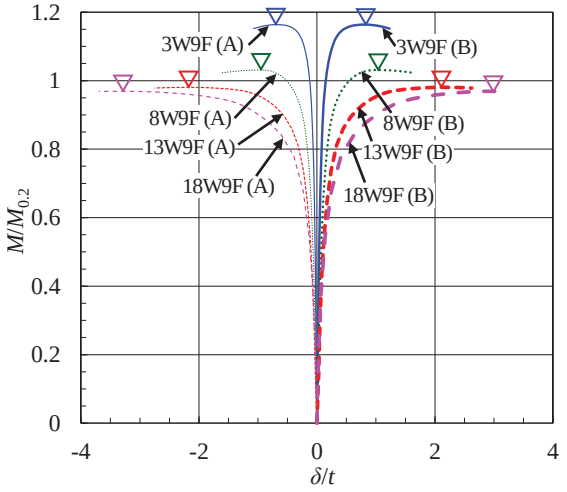

Fig.9 Moment-displacement curves

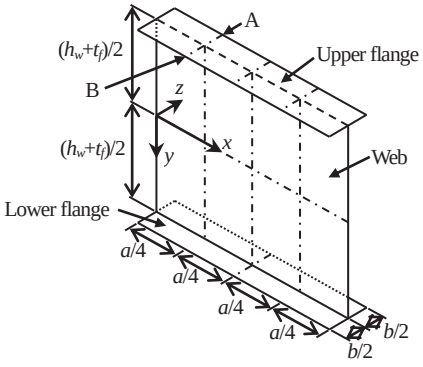

Fig.10 Location of point A and B

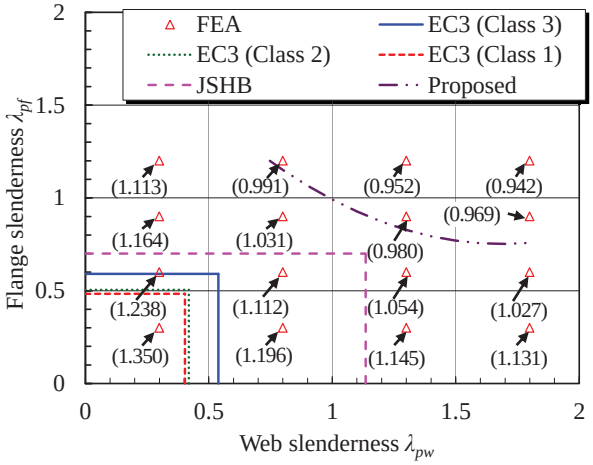

Fig.11 Slenderness parameters and ultimate flexural strength

5. Conclusions

In this study, the effects of the web and flange non-dimensional slenderness parameter on the ultimate flexural behavior and strength of SUS821L1 welded I-section were evaluated through FEA. In addition, the design flexural strength based on rules specified in existing design standards were compared with the ultimate flexural strength obtained from the FEA. Furthermore, the web and flange non-dimensional slenderness parameters were compared with limiting slenderness parameters specified in the standards. The obtained results can be summarized as follows:

(1) Moment-rotation relations of SUS821L1 welded I-section under uniform bending exhibit smooth curve up to the peak point and collapse gradually because of the rounded stress-strain curve.

(2) SUS821L1 welded I-section under uniform bending has considerably high flexural strength that exceeds the strength based on rules specified in existing design standards.
(3) The element interaction of the web and flanges is observed for SUS821L1 welded I-section under uniform bending.
(4) Limiting slenderness parameters for class 3 section of the web and the flange of duplex stainless steel welded I-section under uniform bending specified in Eurocode 3 are considerably conservative to apply to those of SUS821L1 welded I-section.

In this study, although SUS821L1 welded I-section under uniform bending was modeled by aiming at a panel between vertical stiffeners, it is necessary to clarify its validity and coupling effect with lateral buckling or lateral-torsional buckling through tests. In addition, influence of cross-sectional area ratio of the web and flange, and aspect ratio of the web on ultimate flexural behavior of SUS821L1 welded I-section is not able to clear. It is a future work to clarify these problems.

References

1) T. Miyoshi : Residual stresses of lean duplex stainless steel member with welded I-shaped sections, Proceedings of 71st. annual meeting of Japan Society of Civil Engineers, I-306, pp.611-612, 2016. (in Japanese)
2) T. Miyoshi : Mechanical properties and residual stresses of SUS821L1 welded I-section, Journal of Construction Steel, Vol.24, pp.305-312, 2016. (in Japanese)
3) T. Miyoshi : Effect of stress-strain curve on ultimate compressive strength of lean duplex stainless steel plates, Memoirs of National Institute of Technology, Akashi College, Japan, No.59, pp.7-12, 2017. (in Japanese)
4) T. Miyoshi : An experimental study on the ultimate strength of lean duplex stainless steel H-shaped stub-columns, Journal of structural engineering, Vol.63A, pp.67-77, 2017. (in Japanese)
5) N. Nishimura, F. Ohsaki and T. Hasegawa : Experimental investigation on local buckling strength and limiting width-thickness ratios of steel I-sections in bending, Journal of structural engineering, Vol.37A, pp.135-144, 1991. (in Japanese)
6) T. Miyoshi, Y. Miyazaki and S. Nara : Ultimate strength of duplex stainless steel plates under uniaxial compression, Steel Construction Design and Research, Volume 3, Issue 2, pp.90-99, 2010.
7) European Committee for Standardization, CEN : Eurocode3-Design of steel structures-part1-4 : General rules- Supplementary rules for stainless steels, EN 1993-1-4, 2006.
8) Japan Road Association :Specifications for highway bridges, Part Ⅱ: steel bridges, 2012. (in Japanese)
9) Y. Fukumoto (Ed.) : Guidelines for stability design of steel structures, Subcommittee on stability design committee on steel structures, JSCE, Tokyo, 1987. (in Japanese)
10) H.X. Yuan, Y.Q. Wang, Y.J. Shi and L. Gardner : Residual stress distributions in welded stainless steel sections, Thin-Walled Structures, Vol.79, pp.38-51, 2014.
11) S. P. Timoshenko and J. M. Gere : Theory of Elastic Stability, 2nd. Ed., McGrraw-Hill, 1961.
12) M. A. Crisfield : Non-linear finite element analysis of solids and structures Volume 1, Wiley, 1991.